Title

Cubam receptor-mediated endocytosis in hindgut-derived pseudoplacenta of a viviparous teleost *Xenotoca eiseni*

Running title

Endocytosis in pseudoplacenta of teleost

Authors

Atsuo Iida[1, *], Kaori Sano[2], Mayu Inokuchi[3], Jumpei Nomura[1], Takayuki Suzuki[1], Mao Kuriki[4], Maina Sogabe[4], Daichi Susaki[5], Kaoru Tonosaki[5], Tetsu Kinoshita[5], Eiichi Hondo[1]

Affiliations

1. Department of Animal Sciences, Graduate School of Bioagricultural Sciences, Nagoya University, Tokai National Higher Education and Research System, Nagoya, Aichi, Japan.
2. Department of Chemistry, Faculty of Science, Josai University, Sakado, Saitama, Japan.
3. Department of Aquatic Bioscience, Graduate School of Agricultural and Life Sciences, University of Tokyo, Bunkyo, Tokyo, Japan
4. Department of Regeneration Science and Engineering, Institute for Frontier Life and

Medical Sciences, Kyoto University, Kyoto, Kyoto, Japan.

5. Kihara Institute for Biological Research, Yokohama City University, Yokohama, Kanagawa, Japan.

Correspondence: Atsuo Iida

E-mail: tol2.4682@gmail.com

Keywords

endocytosis, Goodeidae, proteolysis, pseudoplacenta, teleost, viviparity

Summary statement

Here, we report that an endocytic pathway is a candidate for nutrient absorption in pseudoplacenta of a viviparous teleost. The trait may have developed from common intestinal mechanism among vertebrates.

Abstract

Nutrient transfer from mother to the embryo is essential for reproduction in viviparous animals. In the viviparous teleost *Xenotoca eiseni* belonging to the family Goodeidae, the intraovarian embryo intakes the maternal component secreted into the ovarian fluid via the trophotaenia. Our previous study reported that the epithelial layer cells of the trophotaenia incorporate a maternal protein via vesicle trafficking. However, the molecules responsible for the absorption were still elusive. Here, we focused on Cubam (Cubilin-Amnionless) as a receptor involved in the absorption, and cathepsin L as a functional protease in the vesicles. Our results indicated that the Cubam receptor is distributed in the apical surface of the trophotaenia epithelium and then is taken into the intracellular vesicles. The trophotaenia possesses acidic organelles in epithelial layer cells and cathepsin L-dependent proteolysis activity. This evidence does not conflict with our hypothesis that receptor-mediated endocytosis and proteolysis play roles in maternal macromolecule absorption via the trohotaenia in viviparous teleosts. Such nutrient absorption involving endocytosis is not a specific trait in viviparous fish. Similar processes have been reported in the larval stage of oviparous fish or the suckling stage of viviparous mammals. Our findings suggest that the viviparous teleost acquired trophotaenia-based viviparity from a modification of the intestinal absorption system common in vertebrates. This is a fundamental study to understand the strategic variation of the reproductive system in vertebrates.

Introduction

August Krogh wrote, "*For such a large number of problems there will be some animal of choice or a few such animals on which it can be most conveniently studied*" [1]. This study aimed to investigate the molecular mechanism of maternal nutrient absorption in a species-specific pseudoplacenta of a viviparous teleost species belonging to the family Goodeidae.

Viviparity is a reproduction system, whereby the oocyte is fertilized in the female body, and subsequent embryo growth occurs with maternal component supply. Each viviparous animal has acquired processes specialized to the gestation in both the mother and embryo [2]. The placenta and umbilical cords in viviparous mammals are major components of the process for mother-to-embryo material transport [3,4]. Other viviparous components such as the extended yolk sac or pseudoplacenta are known in several viviparous vertebrates, except mammals [5].

The family Goodeidae is a freshwater small teleost distributed in Mexico, which includes approximately 40 viviparous species [6]. They possess trophotaenia, which is a hindgut-derived pseudoplacenta that absorbs the maternal component [7,8]. Trophotaenia is a ribbon-like structure consisting of a single epithelial layer, internal blood vessels, and connective tissues [9,10]. The epithelial cell is like an enterocyte in the intestine. Electron microscopy indicated that microvilli form in the apical side of the cell and intracellular vesicles in the cytoplasm [11]. Since the 1980s, these structures have been believed to be involved in maternal component absorption [12]. The nature of the maternal component was predicted to be proteins or other macromolecules secreted into the serum or ovarian fluids; however, no one has experimentally determined its distinct component [13,14]. Recently, we demonstrated that a yolk protein vitellogenin is

81 secreted into the ovarian lumen of pregnant females, and the intraovarian embryo
82 absorbs the nutrient protein via the trophotaenia using a goodeid species *Xenotoca*
83 *eiseni* [15]. In that study, enterocyte-like microvilli and intracellular vesicles were also
84 observed in the epithelial cells of the trophotaenia. We hypothesized that the epithelial
85 layer cell in the trophotaenia absorbs the maternal protein and/or other components as
86 macromolecules because the ovarian lumen lacks proteolysis activity like the digestive
87 intestine. However, the molecules responsible for the trophotaenia-mediated
88 macromolecule absorption have not been reported.

89 Vacuolated enterocytes involved in macromolecule absorption have also been reported
90 in other vertebrate species, including suckling mammals and stomachless fish [16-18].
91 Park et al. [19] reported that the scavenger receptor complex Cubam (Cubilin-
92 Amnionless) and Dab2 are required for macromolecule uptake in zebrafish juveniles.
93 Furthermore, the conditional knockout of *Dab2* in mice led to stunted growth and severe
94 protein malnutrition at the suckling stage [19]. Based on this report, we discuss the
95 commonality of molecular process for the macromolecule absorption between the
96 intestinal enterocytes and the trophotaenia [15]. However, the molecules responsible for
97 macromolecule absorption in the trophotaenia are still elusive.

98 Here, we report candidate molecules for nutrient uptake and subsequent proteolysis in
99 the trophotaenia of *X. eiseni*. An RNA-Seq for trophoteniae indicated candidate receptor
100 molecules and endocytosis-associated proteases expressed in the trophotaenia.
101 Immunohistochemistry and biochemical assays suggested the presence and functions
102 of the candidate factors in the trophotaenia.

Methods

Animal experiments

This study was approved by the ethics review board for animal experiments at Nagoya University (Approval number: AGR2020028). We sacrificed live animals in minimal numbers under anesthesia according to the institutional guidelines.

Fish breeding

X. eiseni was purchased from Meito Suien Co., Ltd. (Nagoya, Japan). Adult fish were maintained in freshwater at 27 °C under a 14:10-h light: dark photoperiod cycle. Fish were bred in a mass-mating design, and approximately 30 adult fish were maintained for this study. The juveniles were fed live brine shrimp larvae, and the adults were fed Hikari Crest Micro Pellets and ultraviolet-sterilized frozen chironomid larvae (Kyorin Co., Ltd., Himeji, Japan). To accurately track the pregnancy period, the laboratory-born fish were crossed in a pair-mating design, and the mating behavior was recorded.

Sample collection

Fish samples were anesthetized using tricaine on ice before the surgical extraction of tissues or embryos. The obtained samples were stored on ice until subsequent manipulations. In this study, we dissected approximately 10 pregnant females and extracted 15–30 embryos in each operation.

124 *RNA-Seq*

125 Total RNA was extracted from trophotaenae of the 3rd or 4th week of the embryo
126 extracted from the pregnant female using the RNeasy Plus Mini kit (QIAGEN). A total of
127 six samples were obtained from three 3rd week embryos and three 4th week embryos.
128 Next-generation sequencing (NGS) was outsourced to Macrogen Japan Corp. (Kyoto,
129 Japan) using NovaSeq6000 (Illumina, Inc., San Diego, CA, USA). Approximately 60
130 million 150-bp paired-end reads were obtained in each sample. The NGS data was
131 deposited to the DNA Data Bank of Japan (DDBJ, ID: DRA011209). *De novo assembly*
132 and mapping to the reference sequence were performed by CLC Genomics Workbench
133 (Filgen, Inc., Nagoya, Japan). The published transcript sequences of *Poecilia reticulata*
134 (NCBI Genome, ID: 23338) were used as a reference. *P. reticulata* is one of the species
135 related to *X. eiseni* for which the transcript sequences have been published, and it
136 belongs to the order Cyprinodontiformes. The transcript sequences of *X. eiseni* were
137 deposited into the DDBJ. The accession numbers are listed in Table 1.

138

139 *Phylogenetic analysis*

140 Amino acid sequences for Cubn, Amn, or Cathepsin L of *Homo sapiens* (human), *Mus*
141 *musculus* (house mouse), *Danio rerio* (zebrafish), *Oryzias latipes* (medakafish), *P.*
142 *reticulata* (guppy), *Xiphophorus maculatus* (platyfish), and *X. eiseni* were collected from
143 the NCBI protein database (https://www.ncbi.nlm.nih.gov/protein/). Phylogenetic trees
144 were constructed by the neighbor-joining method with 1,000 bootstrap replicates in
145 MEGAX (Ver.10.1.8) software (https://www.megasoftware.net/).

146

147 *Reverse transcription (RT) PCR*

148 Total RNA was extracted from tissues or whole embryos using the RNeasy Plus Mini kit
149 and reverse-transcribed using SuperScript IV reverse transcriptase (Thermo Fisher
150 Scientific). PCR was carried out using KOD-FX-Neo (Toyobo, Osaka, Japan) under the
151 following conditions: 100 s at 94 °C, followed by 32 cycles of 20 s at 94 °C, 20 s at
152 60 °C, 60 s at 72 °C, and 120 s at 72 °C. Primer sequences are listed in Table 1.

153

154 *Antibodies and antiserums*

155 Antiserums against Cubn and Amn were generated in this study. The antigen
156 sequences were 6× His-tagged peptide of 151 amino acids (aas) corresponding to the
157 intermediate region of *X. eiseni* Cubn (Accession#, BCN28455; aa 691–841) and 6×
158 His-tagged peptide of 247 aas corresponding to the C-terminal of *X. eiseni* Amn
159 (Accession#, BCN28456). The experimental procedure has been described in our
160 previous study [15]. All antibodies and antiserums used in this study are listed in Table
161 S1.

162

163 *Immunohistochemistry*

164 Tissue samples were fixed in 4.0% paraformaldehyde/phosphate-buffered saline
165 (PFA/PBS) at 4 °C overnight. Samples were permeabilized using 0.5% TritonX-100/PBS
166 at room temperature for 30 min. Endogenous peroxidase was inactivated by 3.0 %
167 hydrogen peroxide/PBS for 10 min. Then, the sample was treated with Blocking-One
168 solution (Nacalai Tesque, Kyoto, Japan) at room temperature for 1 h. Primary antibody

169 or antiserums were used at 1:500 dilution with Blocking-One solution. Samples were
170 incubated with primary antibody or antiserum at 4 °C overnight. Secondary antibodies
171 were used at a 1:500 dilution in 0.1% Tween-20/PBS. Samples were treated with the
172 secondary antibody solution at 4 °C for 2 h. We performed a 3,3'-Diaminobenzidine
173 Tetrahydrochloride (DAB) color development using the DAB Peroxidase Substrate Kit,
174 ImmPACT (Vector Laboratories, Inc., Burlingame, CA, USA). Microscopic observation
175 was performed using an Olympus BX53 microscope and photographed using a DP25
176 digital camera (Olympus, Shinjuku, Japan).

177

178 *Fluorescent Immunohistochemistry*

179 Tissue samples were fixed in 4.0% PFA/PBS at 4 °C overnight. Samples were
180 permeabilized using 0.5% TritonX-100/PBS at room temperature for 30 min.
181 Endogenous peroxidase was inactivated by 3.0 % hydrogen peroxide/PBS for 10 min.
182 Then, the sample was treated with Blocking-One solution (Nacalai Tesque, Kyoto,
183 Japan) at room temperature for 1 h. Primary antibody (anti-Cubn) was used at a 1:500
184 dilution with Blocking-One solution. Samples were incubated with primary antibody at
185 4 °C overnight. Secondary antibody was used at a 1:500 dilution in 0.1% Tween-20/PBS
186 with 4',6-diamidino-2-phenylindole (DAPI). Samples were treated with the secondary
187 antibody solution at 4 °C overnight. Microscopic observation was performed using a
188 Leica TCS SP8 microscope (Leica Microsystems, Wetzlar, Germany).

189

190 *Immunoelectron microscopy*

191 Embryo samples were fixed in 4.0% PFA/PBS. Fixed samples were washed in PBS,
192 then reacted with a primary antibody (anti-Cubn) at 4 °C overnight, and then reacted
193 with biotinylated anti-rabbit IgG (Vector, Burlingame, CA, USA) at room temperature for
194 2 h. Samples were performed with the avidin–biotin–peroxidase complex kit (Vector),
195 and visualized with 0.05% DAB (Dojindo Laboratories, Kumamoto, Japan) and 0.01%
196 hydrogen peroxide in 50 mM Tris buffer (pH 7.2) at room temperature for 10 min. The
197 procedure for electron microscopy is described in our previous study [15].

198

199 *Labeling acidic organelles*

200 The live embryos immediately after extraction from the pregnant female at the 4th-week
201 post-mating were incubated in PBS with a 1:1000 dilution of LysoTracker® Red (Thermo
202 Fisher Scientific) for 1 h at room temperature. The samples were fixed with 4.0 %
203 PFA/PBS and stained with DAPI. Microscopic observation was performed using a Leica
204 DM5000 B microscope (Leica Microsystems, Wetzlar, Germany).

205

206 *Measurement of Cathepsin L activity*

207 The trophotaenia lysate was prepared from six littermate embryos obtained from the
208 pregnant females at the 4th-week post-mating. The trophotaeniae were manually
209 extracted from the embryo under a microscope. Proteolysis detection was performed
210 using the Cathepsin L Activity Fluorometric Assay Kit (BioVision, Inc., Milpitas, CA,
211 USA). The fluorescence intensities were measured using a Qubit 4 Fluorometer
212 (Thermo Fisher Scientific).

213

Results

Gene expression in trophotaenia

Our previous findings and the hypothesis based on that are described in Figure 1A. In a viviparous teleost, *X. eiseni*, the embryo is raised in the ovary while receiving maternal nutrients. The trophotaenia is a pseudoplacenta that plays a role in the absorption of maternal nutrients consisting of proteins and other supplements. Based on previous studies, we hypothesized that several maternal proteins are absorbed by endocytosis-mediated proteolysis in the epithelial cells of the trophotaenia. To verify this hypothesis, we explored candidate genes for receptor, adaptor, vesicle, and protease proteins that are highly expressed in the trophotaenia. RNA-Seq analyses were performed using total RNA extracted from the trophotaeniae of the 3rd- or 4th-week embryos (Figure 1B). We selected candidate genes and compared their predicted expression level as transcription per million (TPM) values that were calculated using the known transcript sequence of *P. reticulata* as reference. RNA-Seq suggested that *cubilin* (*cubn*) and *amnionless (amn*) were highly expressed in the trophotaeniae; however, other co-receptor genes (*lrp1aa*, *lrp2a*) were considerably lower (Figure 1C, Table 2). Adaptor protein-2 (AP2) subunit genes (*ap2a1*, *ap2b1*, *ap2m1a*, and *ap2s1*) were more highly expressed than the other family adaptor genes (*ldlrap1b* and *numb*) (Figure 1C, Table 2). Two families of the vesicle coating protein genes (*clta*, *cltbb*, *cltc*; *flot1b*, *flot2a*) were expressed higher than the vesicle proteins classified in other families (*cav2* and *cav3*) (Figure 1C, Table 2). The lysosomal endopeptidase enzyme gene (*ctsl.1*) exhibited a high TPM value (> 10,000) rather than that of not only protease family genes but also most of the genes expressed in the trophotaeniae (Figure 1C, Table 2). In this investigation, we assumed that the 3rd week is a good growth period (mid pregnancy) and that the 4th week is a poorer growth (late pregnancy) period; thus, we expected that the transcriptomes related to the nutrient

239 transport would vary between these stages. However, the trend of the predicted TPM
240 values in most of the selected genes was not noticeably different between the samples.
241 In the 4th week, only one *clathrin* and four *cathepsin genes* were significantly higher than
242 levels in the 3rd week (Figure 1C).

243

244 *Sequences for Cubam receptor genes*

245 A Cubam receptor is known to be a membrane-bound multi-ligand receptor consisting
246 of Cubn and Amn (Figure 2A). The secreted protein Cubn specifically binds to the
247 transmembrane protein Amn; thus, the CUB domain that associates with the ligands are
248 localized on the apical surface of the plasma membrane. We obtained the amino acid
249 sequences of *X. eiseni* Cubn and Amn by *de novo* assembly of NGS reads from the
250 trophotaeniae. The assembled sequences of *X. eiseni* were calculated to be close to the
251 orthologous sequences of *P. reticulata* and *X. maculatus* (Figure 3A and B). The
252 sequences of Cubn and Amn were compared among four vertebrate species, *H.*
253 *sapiens*, *D. rerio*, *P. reticulata*, and *X. eiseni.* The binding motifs were conserved among
254 the species (Figure 2B and C). A phenylalanine-any-asparagine-proline-any-
255 phenylalanine (FXNPXF) amino acid sequence in the intracellular domain of Amn is
256 known to be a conserved motif used to bind adaptor proteins. The motifs were also
257 conserved among the species (Figure 2D).

258

259 *Distribution of Cubilin and Amnionnless in trophotaenia*

260 To validate the expression of *cubn* and *amn* in the trophotaenia, semi-quantitative RT-
261 PCR analyses were performed using total RNAs extracted from the whole-embryo

262 including the trophotaeniae, isolated trophotaeniae, and adult skeletal muscle. The
263 muscle sample was used as a control for tissue with low endocytosis activity. The gene
264 expression patterns did not conflict between the results of RT-PCR and RNA-Seq. In the
265 embryo and trophotaenia, both *cubn* and *amn* were more highly expressed than *lrp2a*
266 (Figure 4A). Conversely, no or few expressions of the target genes except *actb* as a
267 positive control were detected in the adult muscle. Next, to detect protein localization,
268 immunohistochemistry was performed using antibodies against Cubn or Amn. In both
269 proteins, strong signals were observed in the epithelial monolayer of the trophotaenia,
270 while few background noises were detected in the control assay (Figure 4B-F, see also
271 Figure S1 and S2). Confocal microscopy revealed the cellular distribution of the anti-
272 Cubn signals. The signals in the apical surface of the epithelial cell were detected as a
273 homogeneous distribution, while almost all signals in the cytoplasm were captured as a
274 dot pattern (Figure 4G, Figure S3). Immunoelectron microscopy revealed that the
275 microvilli were distributed on the apical surface of the trophotaenia epithelium, and
276 intracellular vesicles were observed in the cytoplasm; furthermore, anti-Cubn signals
277 were distributed in the intracellular vesicles and overlapped with the microvilli on the
278 apical surface (Figure 4H).

279

280 *Proteolysis activity in trophotaenia*

281 Cathepsin L is a lysosomal cysteine proteinase characterized by three conserved
282 protease regions and active sites consisting of cysteine, histidine, or asparagine (Figure
283 5A). The functional regions were conserved in the *X. eiseni* Cathepsin L protein
284 translated from the coding sequence of *ctsl.1*. The whole amino acid sequence of *X.*
285 *eiseni* Cathepsin L was calculated to be close to the orthologous proteins of *P. reticulata*

286 and *X. maculatus* (Figure 3C). RT-PCR analysis revealed strong expression of *ctsl.1* in
287 trophotaenia (Figure 5B). To identify the type of cells that have proteolysis activity in
288 trophotaenia, acidic organelles including lysosomes and endosomes were detected
289 using a fluorescent probe. LysoTracker® analysis indicated the presence of acidic
290 organelles in the epithelial layer cells (Figure 5C). The signals were distributed in the
291 cytoplasm and were not components of the nuclei (Figure 5D). According to the RNA-
292 Seq analysis, *ctsl.1* was presumed to be the highest expressed *cathepsin* gene in
293 trophotaenia; thus, we calibrated the proteolysis activity of cathepsin L in trophotaenia
294 using a fluorescent substrate-based measurement system. The fluorescence, indicating
295 substrate digestion, was significantly higher in the trophotaenia lysate than in the control
296 at 1 h after reagent mixing. Furthermore, the intensity for the lysate continued to
297 increase for 7 h (Figure 5E, Table 3). Conversely, the increase in intensity was strongly
298 suppressed by a cathepsin L inhibitor. The fluorescent values at each timepoint were
299 statistically different from each other.

300

301 *Adaptors and vesicle coating proteins*

302 The expression of candidate genes for adaptors (*ap2a1*, *ap2b1*, *ap2m1a*, *ap2s1*,
303 *ldlrap1b*, and *numb*) and vesicle coating proteins (*clta* and *cltc*) were confirmed by RT-
304 PCR (Figure 6). We determined an incomplete transcript for *X. eiseni* Dab2 from the *de*
305 *novo* assembly; however, it lacked internal sequences in comparison with the proteins in
306 other vertebrates (Figure S4). Furthermore, no amplicons were obtained by RT-PCR
307 using primers designed based on the Dab2-like sequence.

308

309 **Discussion**

310 RNA-Seq analyses revealed high expression of the genes for receptor-mediated
311 endocytosis in the trophotaenia of *X. eiseni* embryos. Cubn and Amn form a Cubam
312 receptor complex that associates with Vitamin-B12, albumin, transferrin, and other
313 ligands [20,21]. The predicted amino acid sequences for *X. eiseni* Cubn and Amn
314 obtained from the *de novo* assembly both possessed a conserved motif which allowed
315 binding to each other, and Amn retained adaptor binding sites in the intracellular region
316 [21, 22]. Immunohistochemical analysis indicated the presence of Cubn not only in the
317 apical surface of the epithelial layer but also in the intracellular vesicles in the cells,
318 suggesting the incorporation and recycling of endocytic receptors [23,24]. This evidence
319 supports the idea that Cubam plays a role as a receptor for the intraovarian nutrients
320 and is involved in endocytosis. We also indicated the low presence of Lrp2 (also known
321 Megalin), which is a major co-receptor for Cubam [25]. This indicated that Cubam works
322 independently or in cooperation with other co-receptors, except Lrp2, in the
323 trophotaenia. In zebrafish, a previous study reported that Cubam-dependent
324 endocytosis in the lysosome rich enterocytes (LREs) does not require the presence of
325 Lrp2 [19]. This supports our hypothesis; however, we do not exclude the possibility that
326 our sequencing and alignment processes could not catch other *lrp2* orthologous genes
327 in *X. eiseni*. Park et al. [19] also reported that Dab2 is an essential adaptor molecule not
328 only in the zebrafish larval intestine but also in the endocytic nutrient absorption in the
329 ileum of suckling mice. However, we obtained only an incomplete sequence for the *X.*
330 *eiseni* Dab2-like protein without an internal region compared with mammalian orthologs.
331 This may be an alternative splice form with less endocytic activity [26,27]. Furthermore,
332 we did not detect Dab2-like expression by RT-PCR, and we could not exclude the
333 possibility that the predicted Dab2-like sequence is caused by an assembly error. Thus,

334 the contribution of Dab2 to endocytosis in the trophotaenia has not been confirmed in
335 this study. The other adaptor or vesicle coating proteins we detected were typical co-
336 factors for receptor-mediated endocytosis. Conversely, Caveolin is a vesicle coating
337 protein involved in receptor-independent endocytosis [28]. Thus, a low expression of
338 *caveolin* genes (*cav2* and *cav3*) does not conflict with the activation of Cubam-mediated
339 endocytosis. Additionally, biochemical assays supported that cathepsin L is an active
340 protease that functions in the intracellular vesicles that is configured following
341 membrane budding. This evidence supports the idea that Cubam-mediated endocytosis
342 and cathepsin L-dependent proteolysis is one of the key mechanisms for the absorption
343 of the maternal component in *X. eiseni* embryos.

344 Cubam is also known to be a scavenger receptor involved in nonspecific protein uptake
345 [20]. In this study, we did not determine the Cubam ligands in the trophotaenia.
346 However, the candidates are limited to intraovarian secreted proteins. In several
347 goodeid species, previous studies indicated that the ovarian fluids include various
348 proteins in a pattern similar to that in the blood serum [13,29]. Therefore, several serum
349 proteins, albumen, transferrin, and others known as Cubam ligands, are potential targets
350 in the case of intraovarian nutrient absorption via the trophotaenia. Another possibility is
351 that vitellogenin is also a potential target because it is secreted into the ovarian fluids
352 and is absorbed into the trophotaenia via intracellular vesicles [15]. Another study
353 suggested that the Cubn-Amn-Lrp2 receptor complex is related to transport of yolk
354 proteins, including vitellogenin, in endodermal epithelial cells during chicken yolk sac
355 growth [30]. These reports support the idea that Cubn and Amn are potent candidate
356 molecules for a receptor complex involved in maternal component uptake in the
357 trophotaenia. However, functional analyses such as gene knockout or transgenic
358 technologies used in conventional model animals, such as laboratory mice or small

359 oviparous fish, have not been applied to goodeid fish. For a direct validation of our
360 hypothesis, these reverse genetic methods should also be developed in the viviparous
361 teleost.

362 As described above, endocytosis-mediated nutrient absorption is not limited to the
363 pseudoplacenta of the viviparous fish; it has also been reported in intestinal tissues
364 (Figure 7). In mammals, macromolecule absorption in the intestine is limited to the
365 suckling period [31]. In the stomachless fish, endocytosis-mediated absorption is
366 considered to continue in part of the intestine for life, because of low digestive activity in
367 the enteric cavity [18]. We found that Cubn and Amn are also distributed in the intestinal
368 epithelial cells of adult *X. eiseni.* (Figure S5). In most invertebrate species, because the
369 extracellular digestive system is primitive, food particles are absorbed into the intestinal
370 cells by vesicle trafficking and degraded by intracellular digestion [32, 33]. Thus, we
371 hypothesize that endocytic nutrient absorption and intracellular digestion are ancestral
372 traits common not only in vertebrates but also in invertebrates, and their importance has
373 decreased in certain vertebrates with development of the extracellular digestive system
374 in the enteric cavity. The ancestor of the goodeid species may have applied the
375 endocytic process to the reproductive system, and then configured the unique hind-gut
376 derived pseudoplacenta for matrotrophic nutrition during gestation [7,34]. To validate our
377 hypothesis, further exhaustive omics analyses using the goodeid species and
378 comparative research using the subfamily Empetrichthyinae, which is the oviparous
379 species most closely related to the viviparous goodeid fish, are required [6,35].

380 This study is an investigation of species-specific traits based on the transcriptome of a
381 non-conventional model species. The results revealed potential candidate molecules for
382 nutrient absorption in the pseudoplacenta of the viviparous teleost. As August Krogh
383 wrote, this kind of study would be suitable for investigation using the most appropriate

species and is unsuitable for verification using alternative models such as viviparous rodents or oviparous teleosts. We believe that this study is an important and fundamental step in understanding the strategic variation of the reproductive system in vertebrates.

Acknowledgments

This work was supported by research grants from the Nakatsuji Foresight Foundation and the Daiko Foundation.

Competing interest statement

The authors declare that they have no competing interests.

Data accessibility

The data that support the findings have been provided with the manuscript.

References

1. A. Krogh, The progress of physiology. *Am. J. Physiol*. **90**, 243-251 (1929).

2. D. Blackburn, “Viviparity and oviparity: Evolution and reproductive strategies” in: Encyclopedia of Reproduction, Vol. 4, E. Knobil, J. D. Neill, Eds. (Academic Press, 1999), pp. 994-1003.

3. G. J. Burton, A. L. Fowden, Review: The placenta and developmental programming: balancing fetal nutrient demands with maternal resource allocation. *Placenta*. **33**, S23-S27 (2012).

4. R. W. Gill, G. Kossoff, P. S. Warren, W. J. Garrett, Umbilical venous flow in normal and complicated pregnancy. *Ultrasound Med. Biol*. **10**, 349-363 (1984).

5. R. M. Roberts, J. A. Green, L. C. Schulz, The evolution of the placenta. Reproduction (Cambridge, England), **152**, R179–R189 (2016).

6. K. L. Foster, K. R. Piller, Disentangling the drivers of diversification in an imperiled group of freshwater fishes (Cyprinodontiformes: Goodeidae). *BMC Evol. Biol.* **18**, 116 (2018).

7. C. L. Turner, Pericardial sac, trophotaeniae, and alimentary tract in embryos of goodeid fishes. *J. Morphol.* **67**, 271-289 (1940).

8. S. M. Tinguely, A. Lange, C. R. Tyler, Ontogeny and Dynamics of the Gonadal Development, Embryogenesis, and Gestation in *Xenotoca eiseni*

(Cyprinodontiformes, Goodeidae). *Sex Dev*. **13**, 297-310 (2019).

9. C. L. Turner, Viviparity Superimposed upon Ovo-Viviparity in the Goodeidae, a Family of Cyprinodont Teleost Fishes of the Mexican Plateau. *J. Morphol.* **55**, 207- 251 (1933).

10. C. L. Turner, The trophotaeniae of the goodeidae, a family of viviparous cyprinodont fishes. *J. Morphol*. **61**, 495- 523 (1937).

11. J. Lombardi, J. P. Wourms, The trophotaenial placenta of a viviparous goodeid fish. I. Ultrastructure of the internal ovarian epithelium, the maternal component. *J. Morphol*. **184**, 277-292 (1985).

12. F. Hollenberg, J. P. Wourms, Ultrastructure and protein uptake of the embryonic trophotaeniae of four species of goodeid fishes (Teleostei: Atheriniformes). *J. Morphol*. **219**, 105-129 (1994).

13. F. Hollenberg, J. P. Wourms, Embryonic growth and maternal nutrient sources in goodeid fishes (Teleostei: Cyprinodontiformes). *J. Exp. Zool.* **271**, 379–394 (1995).

14. A. Vega-López, E. Ortiz-Ordóñez, E. Uría-Galicia, E. L. Mendoza-Santana, R. Hernández-Cornejo*, et al.,* The role of vitellogenin during gestation of *Girardinichthys viviparus* and *Ameca splendens*; two goodeid fish with matrotrophic viviparity. *Comp. Biochem. Physiol. Part A Mol. Integr. Physiol*. **147**, 731–742 (2007).

15. A. Iida, H. N. Arai, Y. Someya, M. Inokuchi, T. A. Onuma, *et al*., Mother-to-embryo vitellogenin transport in a viviparous teleost *Xenotoca eiseni*. *PNAS*, **116**, 22359-22365 (2019).

16. J. P. Kraehenbuhl, C. Bron, C., B. Sordat, Transfer of humoral secretory and cellular immunity from mother to offspring. *Curr. Top. Pathol*. **66**, 105–157 (1979).

17. P. C. Moxey, J. S. Trier, Development of villus absorptive cells in the human fetal small intestine: a morphological and morphometric study. *Anat. Rec*. **195**, 463–482 (1979).

18. J. H. Rombout, C. H. Lamers, M. H. Helfrich, A. Dekker, J. J. Taverne-Thiele, Uptake and transport of intact macromolecules in the intestinal epithelium of carp (*Cyprinus carpio L.*) and the possible immunological implications. *Cell Tissue Res*. **239**, 519-530 (1985).

19. J. Park, D. S. Levic, K. D. Sumigray, J. Bagwell, O. Eroglu, *et al*., Lysosome-Rich Enterocytes Mediate Protein Absorption in the Vertebrate Gut. *Dev. Cell.* **51**, 7-20 (2019).

20. P. J. Verroust, H. Birn, R. Nielsen, R. Kozyraki, E. I. Christensen, The tandem endocytic receptors megalin and cubilin are important proteins in renal pathology. *Kidney Int*. 62, 745-756 (2002).

21. G. A. Pedersen, S. Chakraborty, A. L. Steinhauser, L. M. Traub, M. Madsen, AMN

477 directs endocytosis of the intrinsic factor-vitamin B(12) receptor cubam by
478 engaging ARH or Dab2. *Traffic*. **11**, 706-720 (2010).
479
480 22. C. Larsen, A. Etzerodt, M. Madsen, K. Skjødt, S. K. Moestrup, C. B. F. Andersen,
481 Structural assembly of the megadalton-sized receptor for intestinal vitamin B12
482 uptake and kidney protein reabsorption. *Nat. Commun.* **9**, 5204 (2018).
483
484 23. E. I. Christensen, H. Birn, P. Verroust, S. K. Moestrup, Membrane receptors for
485 endocytosis in the renal proximal tubule. *Int. Rev. Cytol*. **180**, 237-284 (1998).
486
487 24. B. D. Grant, J. G. Donaldson, Pathways and mechanisms of endocytic recycling.
488 *Nat. Rev. Mol. Cell Biol*. **10**, 597-608 (2009).
489
490 25. E. I. Christensen, H. Birn, Megalin and cubilin: multifunctional endocytic
491 receptors. *Nat. Rev. Mol. Cell Biol.* **4**, 256-266 (2002).
492
493 26. M. E. Maurer, J. A. Cooper, Endocytosis of megalin by visceral endoderm cells
494 requires the Dab2 adaptor protein. *J. Cell Sci*. **118**, 5345-55 (2005).
495
496 27. C. V. Finkielstein, D. G. Capelluto, Disabled-2: A modular scaffold protein with
497 multifaceted functions in signaling. *Bioessays*. **38**, S45-55 (2016).
498
499 28. T. M. Williams, M. P. Lisanti, The caveolin proteins. *Genome Biol*. **5**, 214 (2004).
500
501 29. J. F. Schindler, Structure and function of placental exchange surfaces in goodeid
502 fishes (Teleostei: Atheriniformes). *J. Morphol*. **276**, 991-1003 (2015).

30. R. Bauer, J. A. Plieschnig, T. Finkes, B. Riegler, M. Hermann, W. J. Schneider, The developing chicken yolk sac acquires nutrient transport competence by an orchestrated differentiation process of its endodermal epithelial cells. *J. Biol. Chem.* **288**, 1088-1098 (2013).

31. V. Muncan, J. Heijmans, S. D. Krasinski, N. V. Büller, M. E. Wildenberg, *et al*., Blimp1 regulates the transition of neonatal to adult intestinal epithelium. *Nat. Commun*. **2**, 452 (2011).

32. P. V. Fankboner, Digestive System of Invertebrates. In book: eLS (2001).

33. V. Hartenstein, P. Martinez, Phagocytosis in cellular defense and nutrition: a food-centered approach to the evolution of macrophages. *Cell Tissue Res*. **377**, 527–547 (2019).

34. M. C. Uribe, H. J. Grier, S. A. Avila-Zúñiga, A. García-Alarcón, Change of lecithotrophic to matrotrophic nutrition during gestation in the viviparous teleost *Xenotoca eiseni* (Goodeidae). *J. Morphol*. **279**, 1336-1345 (2018).

35. R. Van Der Laan, W. N. Eschmeyer, R. Fricke, Family-group names of Recent fishes. *Zootaxa*. **3882**, 1-230 (2014).

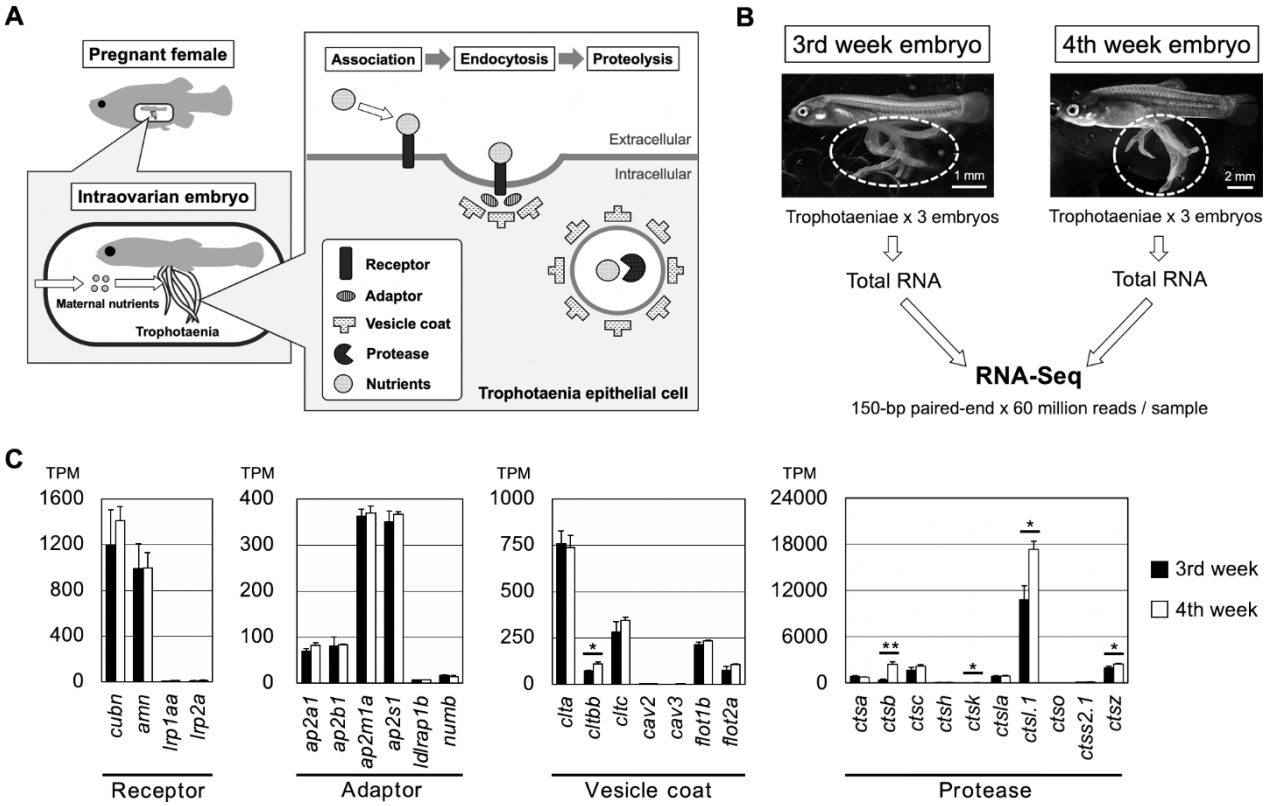

Figure 1. Exploring candidate genes for nutrient absorption

A. A working model and hypothesis of this study. In the goodeid viviparous fish (*X. eiseni*), intraovarian embryo absorbs maternal nutrients via the trophotaenia. We hypothesized that endocytosis-mediated proteolysis is related to nutrient absorption. Based on the scenario, potential target genes are for endocytic receptors, adaptors, vesicle coating proteins, and proteases. **B**. An experimental scheme for the RNA-Seq analysis. RNA samples were obtained from the trophotaeniae (white dotted line) of the single intraovarian embryos extracted from the pregnant females of the 3rd- or 4th-week post-mating. The RNA-Seq was performed using three samples at every stage. **C**. The graphs indicate the transcript per million (TPM) values of the genes selected from the RNA-Seq data that are involved in the endocytosis-mediated proteolysis pathway. Student's *t* test was used for statistical analyses. * $p < 0.05$. ** $p < 0.01$. Error bars represent the standard error.

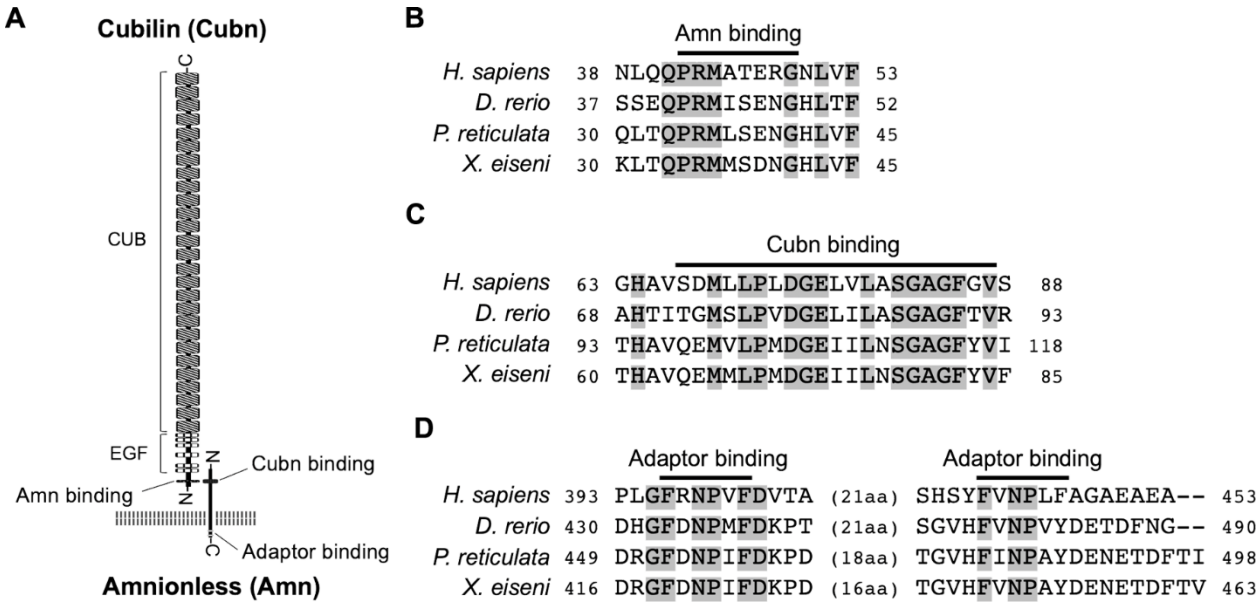

Figure 2. Structures and amino acid sequences for *X. eiseni* Cubn and Amn

A. The illustration indicates that a typical structure of Cubam receptor complex consists of Cubn and Amn. Both proteins possess a conserved motif to bind each other in the N-terminal regions, and the Amn possesses two adaptor binding motifs in the C-terminal intracellular domain. **B-D**. A comparison of amino acid sequence around the Amn-binding motif in Cubn (**B**), Cubn-binding motif in Amn (**C**), and adaptor binding motifs in Amn (**D**) between *X. eiseni* and three other vertebrate species. The gray filled texts are conserved sequences among the four species.

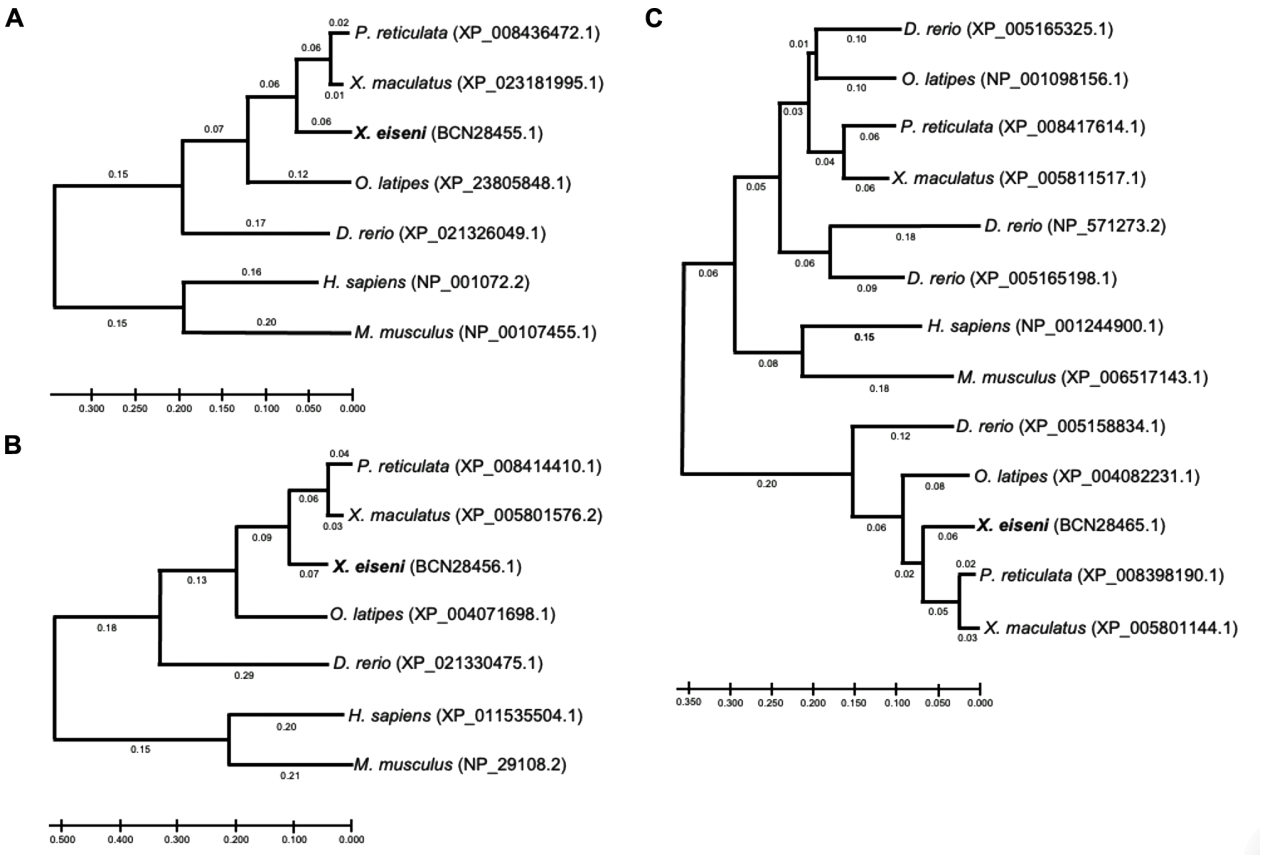

Figure 3. Phylogenetic comparison of Cubn, Amn, and Cathepsin L amino acid sequences

Phylogenetic tree indicating the relationship among the amino acid sequences of Cubn (**A**), Amn (**B**), or Cathepsin L (**C**) in the seven vertebrate species. The sequences of *X. eiseni* (Cyprinodontiformes: Goodeidae) identified in this study were calculated to be closed to the sequences of orthologues in *P. reticulata* and *X. maculatus* (Cyprinodontiformes: Poeciliidae).

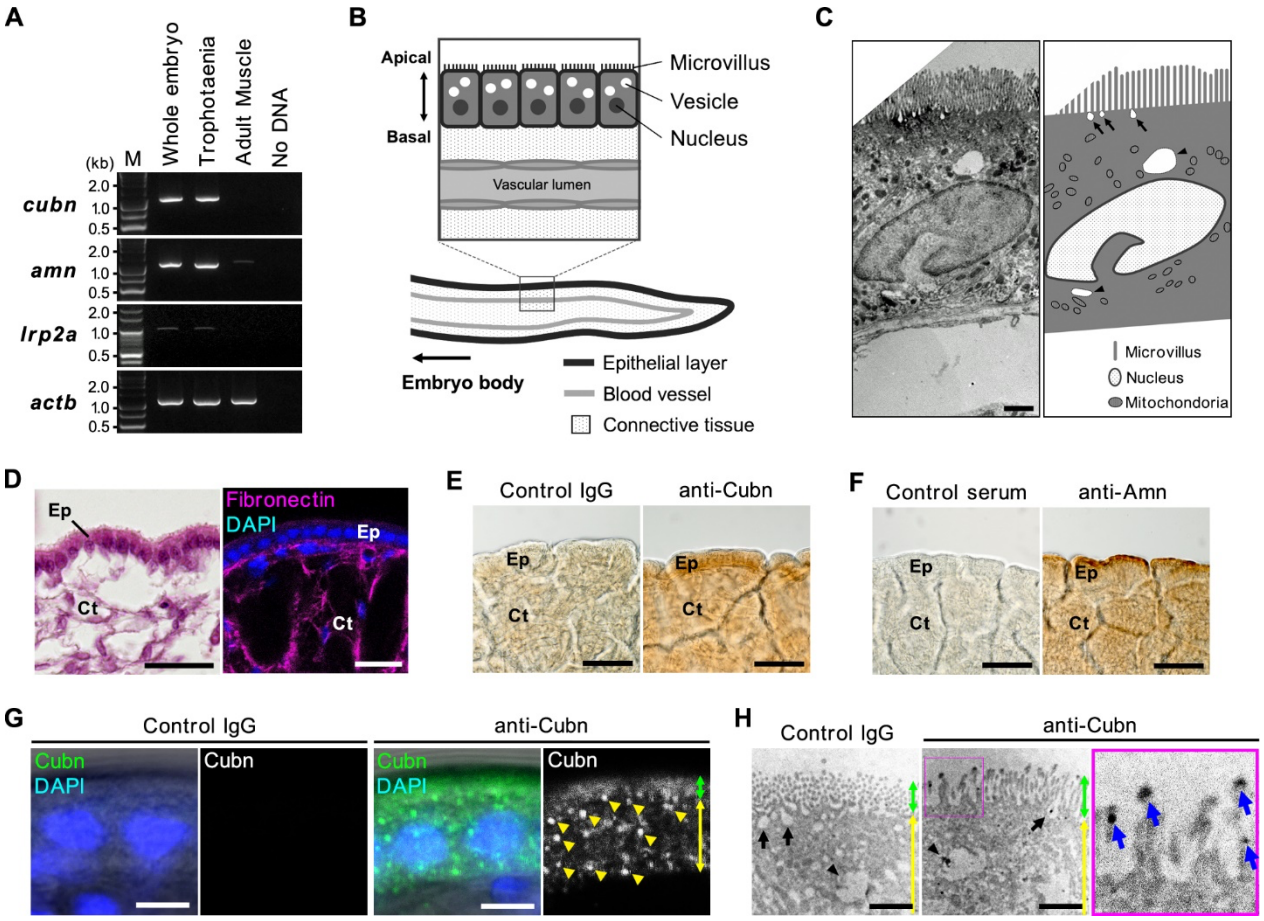

Figure 4. Distribution of receptors involved in endocytosis

A. RT-PCR for the candidate genes for the receptors involved in the endocytosis. All amplicons were detected as single band on the expected sizes based on the transcript sequences obtained from the *de novo* assembly. **B**. The illustration indicates an internal structure of the trophotaenia. An epithelium cell layer configures an outermost structure of the trophotaenia, which contacts the ovarian luminal fluids. The layer consists of an enterocyte-like cell with microvilli on the apical surface and vesicles in the cytoplasm. **C.** Electron microscopy (left) and corresponding illustration (right) of an epithelial layer cell of the trophotaenia. Microvilli are distributed on the apical surface of the cells. Arrows indicate endocytic vesicles during the invagination phase. Arrowheads indicate intracellular vesicles after endocytosis. Scale bar: 1 μm. **D**. The structure of the

573 trophotaeniae stained with HE (left) or fluorescent immunohistochemistry. A fibronectin
574 antibody was used to visualize the connective tissues inside the epithelial layer. Ep,
575 epithelial layer. Ct, connective tissue. Scale bar, 25 μm. **E-F**. Immunohistochemistry
576 using the Cubn antibody or Amn antiserum in the trophotaenia. In both samples, DAB
577 color development was observed in the epithelial layer. Ep, epithelial layer. Ct,
578 connective tissue. Scale bar, 50 μm. **G**. Confocal microscopy images of fluorescent
579 immunohistochemistry using the Cubn antibody in the epithelial layer cells. Yellow
580 triangles indicate the dotted signals in the epithelial cells of the trophotaenia. Green
581 double-headed arrow indicates the apical surface defined by the flat signal. Yellow
582 double-headed arrow indicates the cytoplasmic region including the dotted signals.
583 Scale bar, 5 μm. **H.** Immunoelectron microscopy using the Cubn antibody in the
584 epithelial layer cells. Green double-headed arrow indicates the microvilli on the apical
585 surface. Yellow double-headed arrow indicates the cytoplasmic region including the
586 dotted signals. Arrows indicate endocytic vesicles in the invagination phase. Arrowheads
587 indicate intracellular vesicles after endocytosis. Anti-Cubilin signals were observed in
588 both vesicles. The enlarged image is corresponding to the magenta square focused on
589 the microvilli. Blue arrows indicate anti-Cubn signals in the microvilli. Scale bar, 1 μm.
590

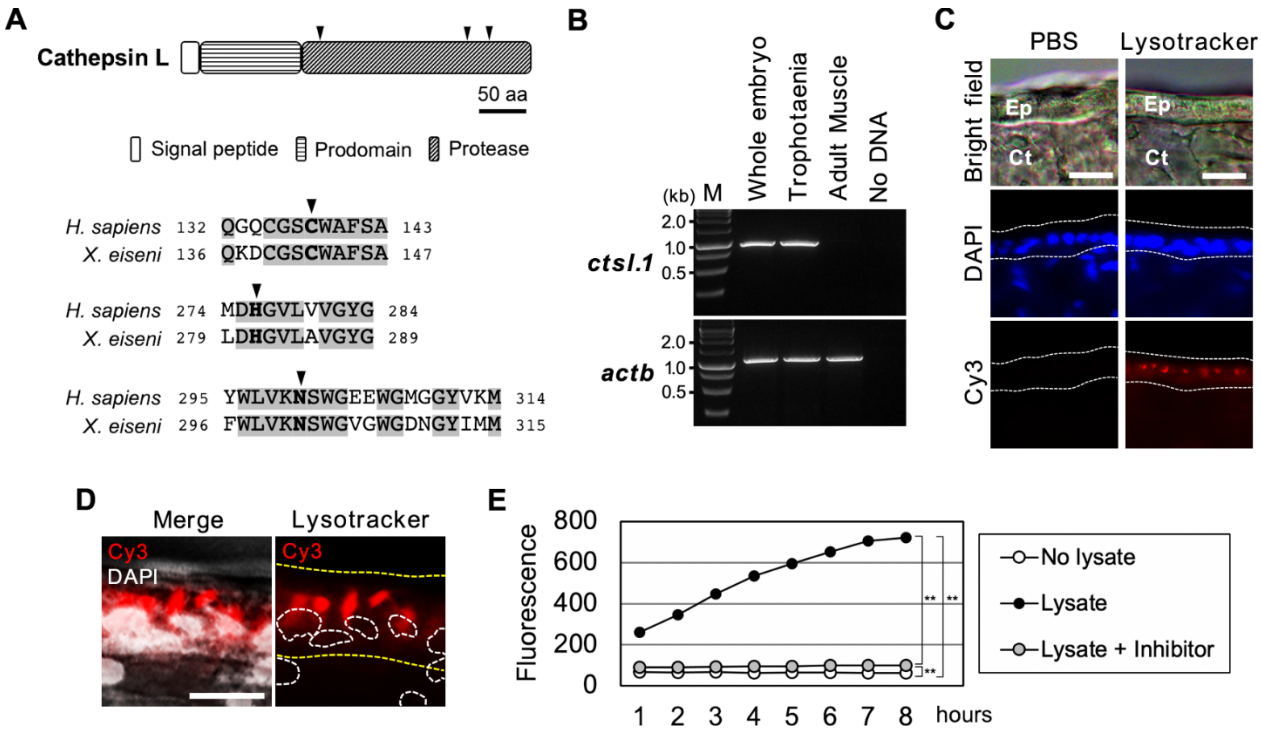

Figure 5. Proteolysis activities in trophotaenia

A. The illustrations indicate a typical structure of cathepsin L and a comparison of the protease domains of cathepsin L between *H. sapiens* and *X. eiseni*. The gray filled texts are conserved sequences among the species. The black triangles indicate protease active sites. **B**. RT-PCR for *cstl.1* exhibited the highest TPM value in the RNA-Seq analysis. The amplicons were detected as a single band on the expected size based on the transcript sequences obtained from the *de novo* assembly. **C**. Labeling of acidic organelles including lysosomal vesicle in the trophotaenia. The lysotracker treatment exhibited red fluorescence in the epithelial layer (white dotted line). Ep, epithelial layer. Ct, connective tissue. Scale bar, 20 μm. **D**. High magnification image of the lysotracker-treated epithelial cell layer of the trophotaenia. Yellow dotted line indicates the epithelial layer and white dotted circles are the nuclei of the epithelial cells. The lysotracker fluorescence was observed in the cytoplasm. Scale bar, 10 μm. **E**. Measurement of

605 cathepsin L activity based on fluorescent substrate degradation. The vertical line
606 indicates the accumulation of cleaved fluorescent substrates, which means cathepsin L
607 activity in the sample solution. The fluorescent value of the trophotaenia lysate sample
608 was increased by 8 h after the reaction started. Student's *t* test was used for statistical
609 analyses. ** $p < 0.01$.
610

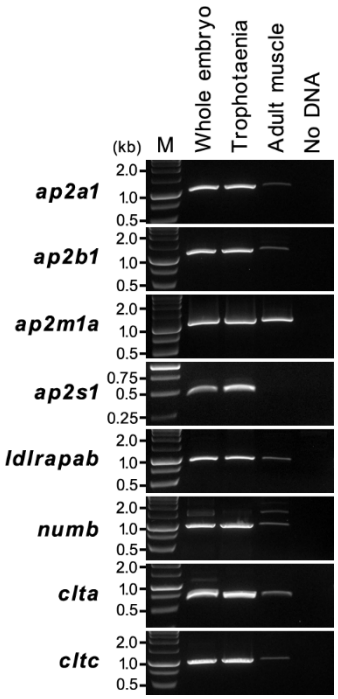

Figure 6. Gene expression analysis of the endocytic adaptor and vesicle coating genes

RT-PCR was performed for the candidate genes encoding the adaptors and vesicle coating genes involved in endocytosis. The amplicons were detected as single bands of the expected sizes based on the transcript sequences obtained from the *de novo* assembly. M, marker.

	Viviparous mammal (*Mus musculus*)	**Stomachless fish** (*Danio rerio*)	**Viviparous fish** (*Xenotoca eiseni*)
			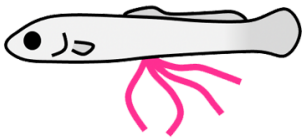
Stage	Suckling	Larva ~ Adult	Intraovarian embryo
Tissue	Intestine (Ileum)	Intestine (LREs)	**Trophotaenia**
Factor	*Dab2*	*cubn*, *dab2*	*cubn*, *amn*, *ctsl.1*
Target	Oral food (Milk)	Oral food (Normal diet)	**Maternal supplement**

Figure 7. Comparison of endocytosis-mediated nutrient intake in vertebrates

Endocytosis-mediated nutrient intake has also been reported in a viviparous mammal and stomachless fish. In these species, oral ingestion macromolecules are absorbed from a region of the intestine via endocytosis. In contrast, intraovarian embryos of the viviparous fish (family Goodeidae) absorbs the maternal component in the ovarian fluids from the trophotaeniae via endocytosis. Endocytosis in each species is predicted to be driven by similar molecular process in the enterocytes of the intestine or the enterocyte-like cells of trophotaenia; however, the biological ontology would be divergent between the viviparous fish (intraovarian growth) and the others (feeding after birth).

Gene	Accession #		Primer sequence (5'-3')	Related figures
cubn	LC595284	F	ATGGCTGTTACAGTGCAGCCTTCA	4A
		R	GGCATGTACATACAGGGAATGCTG	
amn	LC595285	F	TGCCCTTTACAAGCAGTGGATTCC	4A
		R	GCGGATTAGCACAACCACAATCAC	
lrp2a	LC595286	F	ATGTGGAGAACACCGCTGCTTCAA	4A
		R	CCACATGGAGCAGTCATCGAAATC	
ap2a1	LC595287	F	GCTGTGTCGAAGGGAGATGGAATG	6
		R	AGAGCTAGATAGCGCAGATTGGTC	
ap2b1	LC595288	F	GTCATTGCTGCCATGACTGTTGGC	6
		R	CCACAATAGCCTCCTGAACCACAT	
ap2m1a	LC595289	F	GACGTAATGACGGCCTACTTTGGC	6
		R	CAGCAGCGGGTTTCATAGATGCCA	
ap2s1	LC595290	F	ATGATCCGCTTCATCCTCATCCAG	6
		R	CTCTAGTGACTGAAGCATGAGGAG	
ldlrap1b	LC595291	F	GGACGCTTTAAAATCCGCTGGAAG	6
		R	GCAGCTGAGTCTGTCTCATCTTGG	
numb	LC595296	F	GAATAAGCTACGGCAGAGCTTCCG	5
		R	TTGGGCATTGGAGCGGAAGAGAAC	
clta	LC595292	F	GGATGATTTTGACATGCTGAACGC	5
		R	TAACGGACCAGCGGGGACTGCTTT	
cltc	LC595293	F	CTCAGATCCTGCCAATTCGCTTTC	6
		R	TCTTCTTCCACGCAAACAGACAGC	
ctsl.1	LC595294	F	CAGCATCTCTCTGGAAGATCTCGA	5B
		R	CAGACTAGTGGATAACTTGCTGCG	
actb	LC595295	F	ATGGAAGATGAAATCGCCGCACTG	4A, 5B
		R	GAAGCATTTACGGTGGACGATGGA	

631 **Table 1. List of primers used in the study.**

632 F, forward, R, reverse.

		3 weeks				4 weeks			
		#1	#2	#3	**Average**	#1	#2	#3	**Average**
Receptor	***cubn***	1421	768	1414	**1201**	1528	1464	1250	**1414**
	amn	745	966	1269	**993**	1139	818	1032	**996**
	lrp1aa	6	4	10	**7**	14	10	8	**11**
	lrp2a	12	6	10	**9**	12	7	12	**10**
Adaptor	***ap2a1***	75	60	73	**69**	78	89	82	**83**
	ap2b1	91	54	98	**81**	84	83	85	**84**
	ap2m1a	383	346	360	**363**	349	374	385	**369**
	ap2s1	365	318	368	**350**	359	370	371	**367**
Vesicle	***ldlrapab***	7	6	7	**7**	8	8	6	**7**
	numb	19	15	19	**18**	17	15	13	**15**
	clta	851	680	744	**758**	664	739	817	**740**
	cltb	67	76	73	**72**	97	127	104	**109**
	cltc	337	209	308	**285**	328	366	343	**346**
	cav2	1	0	2	**1**	4	2	3	**3**
	cav3	0	0	0	**0**	0	0	0	**0**
	flot1b	229	196	221	**215**	228	238	234	**233**
	flot2a	91	50	89	**77**	228	238	234	**233**
Protease	***ctsa***	862	691	939	**831**	751	749	720	**740**
	ctsb	474	234	429	**379**	2686	2559	1944	**2396**
	ctsc	1867	1113	1907	**1629**	2273	2320	1884	**2159**
	ctsh	52	31	52	**45**	47	55	48	**50**
	ctsk	11	17	14	**14**	24	24	18	**22**
	ctsla	831	736	939	**835**	960	809	924	**898**
	ctsl.1	12749	8412	11227	**10796**	17795	18334	15906	**17345**
	ctso	3	5	7	**5**	6	7	8	**7**
	ctss2.1	2144	1656	2042	**1947**	2494	2500	2342	**2445**
	ctsz	66	63	63	**64**	530	551	523	**535**

633 **Table 2. The TPM values for endocytic genes in the RNA-seq analysis.**

634

		1 h	2 h	3 h	4 h	5 h	6 h	7 h	8 h
No lysate	#1	68.8	67.8	67.2	65.8	65.5	65.8	65.6	65.2
	#2	66.5	65.9	64.8	62.7	64.0	64.4	63.8	62.7
	#3	66.8	65.4	69.8	63.1	63.3	62.8	61.8	62.6
	Average	**67.4**	**66.3**	**67.3**	**63.8**	**64.3**	**64.3**	**63.8**	**63.5**
Lysate	#1	260.3	345.0	437.7	530.4	579.7	637.3	699.6	694.1
	#2	264.9	351.6	460.3	551.3	617.0	678.4	727.0	748.2
	#3	256.6	339.2	441.8	522.7	587.1	642.9	692.5	720.8
	Average	**260.6**	**345.3**	**446.6**	**534.8**	**594.6**	**652.9**	**706.3**	**721.0**
Lysate + inhibitor	#1	94.0	96.2	98.0	99.6	101.0	106.8	104.4	101.9
	#2	88.1	88.8	91.1	91.5	93.4	94.0	98.0	98.2
	#3	88.3	88.4	89.4	93.1	94.2	96.4	99.4	101.0
	Average	**90.1**	**91.2**	**92.8**	**94.7**	**96.2**	**99.0**	**100.6**	**100.4**

635 **Table 3. The measured fluorescent signal values indicating cathepsin L-**

636 **dependent proteolysis.**